Soft Matter

PAPER

View Article Online
View Journal | View Issue

Check for updates

Cite this: *Soft Matter*, 2018, **14**, 8205

Hard convex lens-shaped particles: metastable, glassy and jammed states

Giorgio Cinacchi *[a] and Salvatore Torquato *[b]

We generate and study dense positionally and/or orientationally disordered, including jammed, monodisperse packings of hard convex lens-shaped particles (lenses). Relatively dense isotropic fluid configurations of lenses of various aspect ratios are slowly compressed *via* a Monte Carlo method based procedure. Under this compression protocol, while 'flat' lenses form a nematic fluid phase (where particles are positionally disordered but orientationally ordered) and 'globular' lenses form a plastic solid phase (where particles are positionally ordered but orientationally disordered), 'intermediate', neither 'flat' nor 'globular', lenses do not form either mesophase. In general, a crystal solid phase (where particles are both positionally and orientationally ordered) does not spontaneously form during lengthy numerical simulation runs. In correspondence to those volume fractions at which a transition to the crystal solid phase would occur in equilibrium, a 'downturn' is observed in the inverse compressibility factor *versus* volume fraction curve beyond which this curve behaves essentially linearly. This allows us to estimate the volume fraction at jamming of the dense non-crystalline packings so generated. These packings are nematic for 'flat' lenses and plastic for 'globular' lenses, while they are robustly isotropic for 'intermediate' lenses, as confirmed by the calculation of the τ order metric, among other quantities. The structure factors $S(k)$ of the corresponding jammed states tend to zero as the wavenumber k goes to zero, indicating they are effectively hyperuniform (*i.e.*, their infinite-wavelength density fluctuations are anomalously suppressed). Among all possible lens shapes, 'intermediate' lenses with aspect ratio around 2/3 are special because they are those that reach the highest volume fractions at jamming while being positionally and orientationally disordered and these volume fractions are as high as those reached by nematic jammed states of 'flat' lenses and plastic jammed states of 'globular' lenses. All of their attributes, taken together, make such 'intermediate' lens packings particularly good glass-forming materials.

Received 25th July 2018,
Accepted 24th September 2018

DOI: 10.1039/c8sm01519h

rsc.li/soft-matter-journal

Published on 26 September 2018. Downloaded by Princeton University on 10/22/2018 1:56:48 PM.

I. Introduction

Hard-particle systems are basic model systems with which to investigate (soft) condensed matter.[1] While theoretically interesting, their practical utility rests on the fact that short-range steeply repulsive interactions are the main determinant of the static and dynamic physico-chemical properties of dense molecular systems.[2] In addition, the synthesis of colloidal particles that interact as hard particles has progressed so that they are now available in a variety of shapes and sizes.[3] Such hard-particle colloidal systems exhibit a variety of equilibrium phases, not only fluid and crystalline phases but also plastic- and liquid-crystalline mesophases, and non-equilibrium states, such as glassy states.[4–10] They also play a role in understanding the behaviour of biological macromolecules in biological fluids.[11]

Within this extensive body of work is a recent study of the dense (positionally and orientationally) ordered packings and phase behaviour of systems of hard convex lens-shaped particles (lenses).[12] These hard axially and centrally symmetric disc-like particles, introduced a quarter century ago,[13] correspond to the intersection volume of two congruent (three-dimensional) spheres. By varying either the radius of or the center-to-center distance between these two spheres, lenses can be generated whose shape interpolates between the hard-infinitesimally thin-disc and the hard-sphere models. Lenses can be specified by the aspect ratio $\kappa = b/a$, with a and b respectively the major and minor axes. Equivalently, they can also be specified by $R^* = R/\sigma$, with R the radius of the two spheres and σ^2 the surface area of one of the two constituent spherical caps. Note that $\kappa \in [0,1]$ while $R^* \in \left(1/\sqrt{2\pi}, \infty\right)$, with $\kappa = 0$ or $R^* \to \infty$

[a] *Departamento de Física Teórica de la Materia Condensada, Instituto de Física de la Materia Condensada (IFIMAC), Instituto de Ciencias de Materiales "Nicolás Cabrera", Universidad Autónoma de Madrid, Ciudad Universitaria de Cantoblanco, E-28049 Madrid, Spain. E-mail: giorgio.cinacchi@uam.es*
[b] *Department of Chemistry, Department of Physics, Institute for the Science and Technology of Materials, Program for Applied and Computational Mathematics, Princeton University, Princeton, New Jersey 08544, USA. E-mail: torquato@princeton.edu*

Published on 26 September 2018. Downloaded by Princeton University on 10/22/2018 1:56:48 PM.

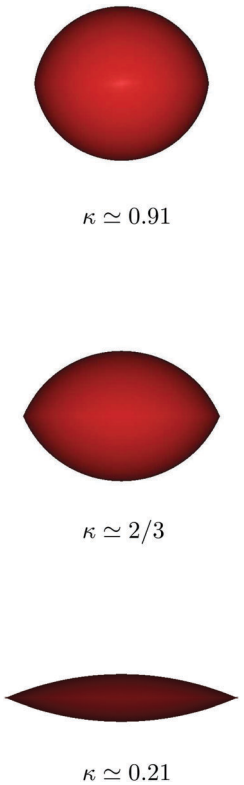

Fig. 1 Depiction of lenses with three different aspect ratios κ: a 'globular' lens with $\kappa \simeq 0.91$, an 'intermediate' lens with $\kappa \simeq 2/3$ and a 'flat' lens with $\kappa \simeq 0.21$.

corresponding to the hard-infinitesimally thin-disc case and $\kappa = 1$ or $R^* = 1/\sqrt{2\pi}$ to the hard-sphere case. Based on their equilibrium phase diagram,[12] lenses can be categorised, with respect to the value of κ, into 'flat', 'intermediate' and 'globular' (Fig. 1). On increasing volume fraction $\phi = \varrho v$, with ϱ the number density and v the particle volume, lenses of the first category exhibit the phase sequence isotropic (I) fluid → nematic[14] (N) fluid → crystalline (C) solid. Instead, lenses of the second category exhibit the phase sequence I fluid → C solid. In turn, lenses of the third category exhibit the phase sequence I fluid → plastic[15] (P) solid → C solid. Despite their shapes and equilibrium phase diagram being very similar to those of hard oblate ellipsoids,[16] the subtle differences between these two hard-particle models manifest at the high ϕ's, most notably through the structure of the densest-known packings (DKP) and the functional form of their volume fraction ϕ_{DKP} as a function of κ.[12] In addition, unlike those of hard (prolate and oblate) ellipsoids,[17] these densest-known packings of lenses are infinitely degenerate,[12] such as the densest packings of hard spheres.[6,10] This intrinsic degeneracy may add to the rotational degrees of freedom to make lenses particularly good glass formers.

In this sequel, we turn our attention to the study of dense (positionally and/or orientationally) disordered packings of lenses. We generate long-lived metastable non-crystalline states by slowly compressing I fluid systems of lenses up to jamming ϕ's while avoiding formation of the thermodynamically stable C solid phase. Indeed, their rotational degrees of freedom and intrinsic degeneracy of dense packings, along with the fact that the I fluid, N fluid and P solid branches are well separated from the C solid branch in the respective $\kappa \to 0$ and $\kappa \to 1$ limits, suggest that, for lenses, the C solid phase avoidance could be achieved even starting from the dense I fluid phase and compressing the system slowly so as to potentially preserve the formation of the two mesophases for ϕ's up to those of the corresponding jammed states. Thus, the structure of the strictly jammed states here generated is nematic (positionally disordered and orientationally ordered) for 'flat' lenses, plastic (positionally ordered and orientationally disordered) for 'globular' lenses, while remains isotropic (positionally and orientationally disordered) for 'intermediate' lenses. Importantly, 'intermediate' lenses with $\kappa \simeq 2/3$ are able to reach values of ϕ at jamming comparable to those reached by 'flat' and 'globular' lenses without the need to separately introduce either positional or orientational orderings.

Out of previous works on dense positionally and orientationally disordered packings of hard non-spherical particles[18–24] several of them[19–21,23,24] focussed on generating and characterising maximally random jammed (MRJ) states, *i.e.*, the states that, among all the jammed states of a system, minimise suitably defined positional and orientational order metrics.[25] Besides their volume fraction ϕ_{MRJ} and low order-metric values, one important characteristic of any hard-particle MRJ state is its hyperuniformity.[26–30] In general, a hyperuniform many-particle system in d-dimensional Euclidean space $\mathbb{R}^d$ is one in which the structure factor $S(\mathbf{k}) \equiv 1 + \varrho\tilde{h}(\mathbf{k})$ tends to zero as the wavenumber $k \equiv |\mathbf{k}|$ tends to zero;[26–29] *i.e.*,

$$\lim_{|\mathbf{k}| \to 0} S(\mathbf{k}) = 0, \tag{1}$$

where $\tilde{h}(\mathbf{k})$ is the Fourier transform of the total correlation function $h(\mathbf{r}) = g(\mathbf{r}) - 1$ and $g(\mathbf{r})$ is the standard pair correlation function. Here, we specifically show that the positionally and orientationally disordered packings of lenses with $\kappa \simeq 2/3$ are effectively hyperuniform. The fact that these strictly jammed packings are hyperuniform in addition to being isotropic makes them good glass formers and promising materials.

In Section II, we describe the Monte Carlo (MC) method[31,32] based compression protocol that we employed along with the set of quantities that were chosen to be calculated to characterise the structure of the generated packings. In Section III, we present all of our results. In Section IV, we summarise them and provide certain concluding remarks.

II. Monte Carlo method based compression protocol and calculated structural indicators

Pure systems of N lenses, N ranging from a minimum of $\simeq 100$ to a maximum of $\simeq 2300$, were considered for several values of R^* hence κ. Well-equilibrated configurations in the dense I fluid phase were taken to start compression runs using the

 This journal is © The Royal Society of Chemistry 2018

Published on 26 September 2018. Downloaded by Princeton University on 10/22/2018 1:56:48 PM.

well-established MC numerical simulation method[31,32] in the isobaric–isothermal (*NPT*) ensemble[33] with variable-shape triclinic computational boxes[34] and periodic boundary conditions, a procedure that is essentially equivalent to a MC implementation of the adaptive-shrinking-cell (ASC) method.[35] The MC runs made sub-divide into two groups.

For 'flat', 'intermediate' and 'globular' lenses, a series of compression runs was carried out in which a MC cycle consisted of a sequence of trial moves on average comprising one computational box's shape and volume move every $2N$ translational or rotational moves, the size of any type of trial move being such to ensure an acceptance rate of 20–30% for each, with dimensionless pressure $P^* = P\sigma^3/k_BT$ increased relatively gently and length being typically of 1–10 million MC cycles.

Especially for lenses with $\kappa > 1/2$ and whenever the aim was to obtain single MRJ configurations, a series of compression runs was also carried out in which a MC cycle was such that the average rate of updating the computational box's shape and volume was increased up to 20 moves every $2N$ translational or rotational moves, always ensuring an acceptance rate of 20–30% for each type of trial move, with P^* increased harshly, typically a factor 10 every 1 million of MC cycles until reaching $P^* = 10^6$.

In the course of all these MC runs, the average over ϱ hence ϕ was calculated along with that over the nematic order parameter[36] S_2 as well as a set of real-space positional and orientational pair correlation functions. This set includes the standard positional pair correlation function $g(r)$ and the second-order orientational pair correlation function $G_2^{\hat{\mathbf{u}}}(r)$ (for a definition of these functions one may consult ref. 12; here suffice it to recall that r is the distance separating the centroids of two lenses and $\hat{\mathbf{u}}$ is the unit vector along a lens' C_∞ symmetry axis) as well as the second-order bond-orientational pair correlation function $G_2^{\hat{\mathbf{r}}}(r)$ defined as:

$$G_2^{\hat{\mathbf{r}}}(r) = \left\langle \frac{\sum_{i=1}^{N}\sum_{j\neq i}^{N} P_2\left(\hat{\mathbf{r}}_{ij}\cdot\hat{n}\right)\delta\left(r-r_{ij}\right)}{\sum_{i=1}^{N}\sum_{j\neq i}^{N}\delta\left(r-r_{ij}\right)}\right\rangle, \qquad (2)$$

with: $\mathbf{r}_{ij}$ the interparticle vector between lens i and lens j centroids, r_{ij} being its modulus and $\hat{\mathbf{r}}_{ij}$ the unit vector defining its orientation; $\hat{n}$ the nematic director;[36] $P_2(x)$ the second-order Legendre polynomial; $\delta(r)$ a radial delta function; and angular brackets $\langle\,\rangle$ indicate an ensemble average. The mathematical analysis of these positional and orientational pair correlation functions could lead to order parameters such as the positional order parameter[37]

$$\tau = \frac{4\pi}{a^3}\int_0^a \mathrm{d}r r^2[g(r)-1]^2, \qquad (3)$$

while the orientational order parameter S_2 could also be obtained as:[38]

$$S_2^2 = \lim_{r\to\infty} G_2^{\hat{\mathbf{u}}}(r). \qquad (4)$$

For the relatively gently compressed systems, the approach to jamming was monitored *via* the ϕ dependence of the inverse compressibility factor $\frac{\varrho}{\beta P}$, progressively acquiring a free-volume-theory[39,40] explained linear behaviour as the glass transition regime had been crossed. While rigorously testable using linear programming, the strictness condition[41] of a final jammed packing, either generated by relatively gentle or harsh compression, was heuristically[42] verified by observing no drift in both the positions and orientations of the constituent hard particles in the course of MC runs at $P^* = 10^6$ as long as 5 million MC cycles.

To investigate the hyperuniformity[26–29] of these strictly jammed packings, we computed the orientationally averaged structure factor $S(k)$ from

$$S(k) = \frac{1}{N}\left\langle \left|\sum_{j=1}^{N} \mathrm{e}^{i\mathbf{k}\cdot\mathbf{r}_j}\right|^2\right\rangle_{\hat{\mathbf{k}}}, \quad \mathbf{k}\neq 0 \qquad (5)$$

where $\{\mathbf{r}_1, \mathbf{r}_2, \ldots, \mathbf{r}_j, \ldots, \mathbf{r}_N\}$ are the particle centroid positions within a fundamental cell under periodic boundary conditions and $\langle\,\rangle_{\hat{\mathbf{k}}}$ indicates the suitable orientational average over each admissible wavevector $\mathbf{k}$ so that S is a function of the wavenumber k.

III. Results

A. 'Flat' lenses

The discussion of the results obtained starts with those relevant to systems of lenses with $\kappa < 1/3$. Thanks to the thinness of these hard convex particles, the I–N phase transition is well-defined, occurring at a relatively low volume fraction, $\phi_{IN} < 0.4$, well below the N–C phase transition. Once formed, the N fluid phase can be compressed further and, based on the above-mentioned assumption on the C solid phase avoidability, this could allow for an exploration of the very dense nematic packing regime.

Fig. 2(a) shows the equation of state, conveniently represented as the inverse compressibility factor $\frac{\varrho}{\beta P}$ *versus* ϕ,[43] for lenses with $\kappa \simeq 0.094$ and $\kappa \simeq 0.29$. Shown are also the data previously obtained for hard infinitesimally thin discs with $\kappa = 0$;[44,45] just for the purpose of comparison, a finite volume equal to that of lenses with $\kappa \simeq 0.028$ has been arbitrarily conferred to these hard infinitesimally thin particles. Within this graphical representation, the weakly first-order I–N phase transition of hard infinitesimally thin discs is signalled by a clear cusp: by virtue of the transition to the orientationally ordered fluid phase, the system compressibility increases and $\frac{\varrho}{\beta P}$ rises with ϕ asymptotically tending to 1/3.[44] Lenses with $\kappa \simeq 0.094$ too are still thin enough to exhibit this cusp at the I–N phase transition but the finite value of their v makes $\frac{\varrho}{\beta P}$ readily decrease with ϕ once having reached a nearby local maximum. Lenses with $\kappa \simeq 0.29$ are already too thick to make both the cusp and the nearby local maximum essentially vanish.

Published on 26 September 2018. Downloaded by Princeton University on 10/22/2018 1:56:48 PM.

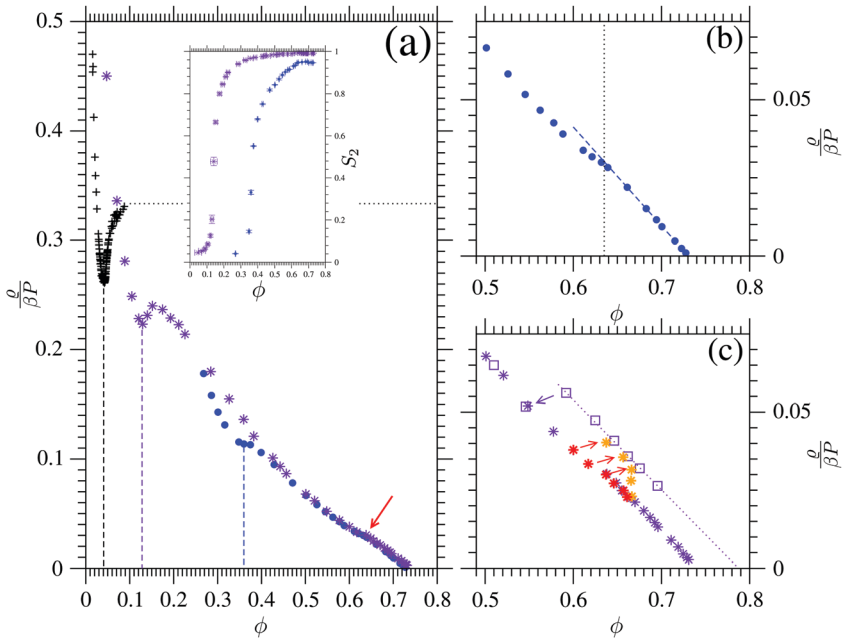

Fig. 2 (a) Inverse compressibility factor $\frac{\varrho}{\beta P}$ as a function of volume fraction ϕ for $\kappa \simeq 0.29$ (blue or dark gray circles), $\kappa \simeq 0.094$ (indigo or dark gray asterisks) and $\kappa = 0$ (black plusses); the three vertical dashed lines approximately locate the respective I–N phase transition while the horizontal dotted line is the asymptote that the $\frac{\varrho}{\beta P}$ *versus* ϕ curve for a system of hard infinitesimally thin discs approaches. The arrow points to those values of ϕ at which the $\frac{\varrho}{\beta P}$ *versus* ϕ curves show a 'downturn'. In the inset: Nematic order parameter S_2 as a function of volume fraction ϕ for systems of lenses with $\kappa \simeq 0.29$ (blue or dark gray circles) and $\kappa \simeq 0.094$ (indigo or dark gray asterisks). (b) Zoom in on the high-volume-fraction regime of $\frac{\varrho}{\beta P}$ *versus* ϕ for $\kappa \simeq 0.29$: the dashed line is a linear fit restricted to values of ϕ larger than 0.65 while the dotted line approximately locates the 'downturn'. (c) Zoom in on the high-volume-fraction regime of $\frac{\varrho}{\beta P}$ *versus* ϕ for $\kappa \simeq 0.094$: shown are also the data for the C solid phase (indigo or dark gray squares) and the corresponding linear fit (dotted line) while red (or gray) and orange (or light gray) asterisks correspond to the initial and final states of lengthy MC runs at $P^* = 300$, 350, 400, 450, 500, 550. Wherever clarity is not too compromised, pairs of long-lived states corresponding to the same value of P^* are joined by an arrow pointing towards the equilibrium phase.

With increasing ϕ, the $\frac{\varrho}{\beta P}$ *versus* ϕ curves for the two finite-v lenses progressively approach one another until they nearly superimpose. It is in this high-volume-fraction regime that both show a 'downturn' at $\tilde{\phi} \sim 0.64$ beyond which $\frac{\varrho}{\beta P}$ decays essentially linearly with ϕ. Based on this free-volume-theory feature, one can extrapolate the value of the nematic state highest volume fraction: $\phi_{\max_N} = 0.745 \pm 0.007$ for $\kappa \simeq 0.094$ and 0.732 ± 0.008 for $\kappa \simeq 0.29$ [Fig. 2(b)].

The trend of S_2 *versus* ϕ reflects that of the equation of state: in correspondence to the 'downturn' at larger values of ϕ, S_2 ceases to increase with ϕ in a typical nematic-like manner, as it does at smaller values of ϕ, but remains essentially stuck at a value $\sim$0.99 for lenses with $\kappa \simeq 0.094$ and a value of $\sim$0.95 for lenses with $\kappa \simeq 0.29$ [Fig. 2(a)].

The observed 'downturns' occur at values of ϕ at which the C solid is the thermodynamically stable phase. It becomes of interest to investigate whether crystallisation does finally occur once much lengthier MC runs have been carried out. This aspect has been particularly investigated for lenses with $\kappa \simeq 0.094$ [Fig. 2(c)].

Fig. 3 shows the evolution of ϕ and S_2 as a function of MC cycles at several values of P^* in the interval [250,550]. One may take 250 as the approximate limit dimensionless pressure below which crystallisation cannot occur. In fact, at $P^* = 250$ both the nematic and crystal states are mechanically stable for as long as 50×10^6 MC cycles while at smaller values of dimensionless pressure, such as 200 and 150, the crystal melts more and more rapidly: at $P^* = 200$ one can observe a 10^6 MC cycle-long metastable crystal transient whereas at $P^* = 150$ the crystal is so unstable that it melts in less than 10^5 MC cycles. In agreement with previous calculations aimed at sketching the lens equilibrium phase diagram,[12] it is seen that at $P^* = 300$, 350 and (partly) 400 the C solid phase does form starting from a nematic configuration: one can see the good agreement with the C solid phase equation of state previously determined on decompressing from the densest-known orthorhombic configuration.[12] (One can note that S_2 too remains an indicator of this phase transition.) However, crystallisation coarsens as the dimensionless pressure rises to 450: at this value of P^*, it was not possible to reach the same value of ϕ characteristic of a well-defined crystal. For values of P^* still larger, crystallisation appears inhibited. The 'downturn' in the $\frac{\varrho}{\beta P}$ *versus* ϕ curve shows up in correspondence to these values of dimensionless pressure at which full crystallisation has failed to occur. Fig. 3 also shows that crystallisation 'time'-scale much depends on the system size. Taking $P^* = 350$ as an example, crystallisation is

 This journal is © The Royal Society of Chemistry 2018

Published on 26 September 2018. Downloaded by Princeton University on 10/22/2018 1:56:48 PM.

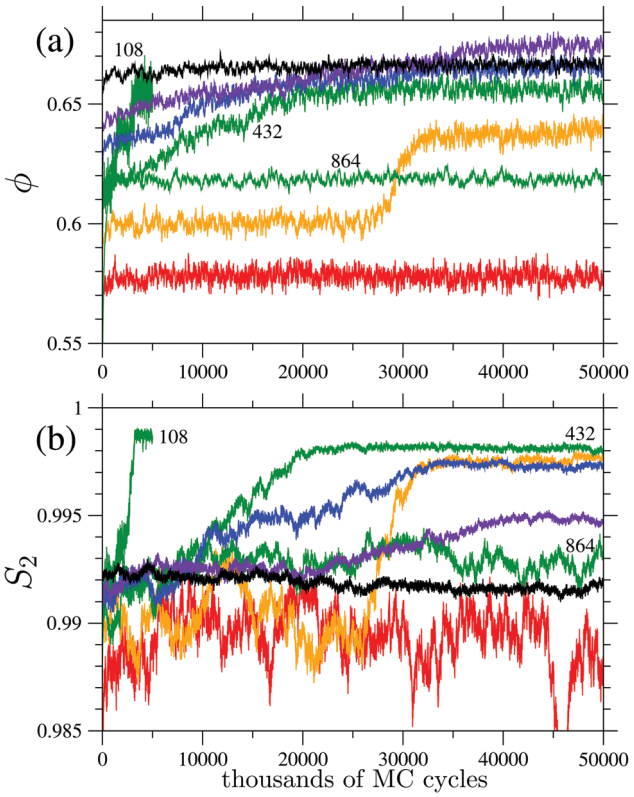

Fig. 3 The evolution of volume fraction ϕ (a) and nematic order parameter S_2 (b) during lengthy MC runs for a system of lenses with $\kappa \simeq 0.094$ at several values of dimensionless pressure P^*: 250 (red or gray); 300 (orange or light gray); 350 (green or gray); 400 (blue or dark gray); 450 (indigo or dark gray); 550 (black). Note that at $P^* = 350$ there are three curves labelled by the number N used: 108, 432, 864.

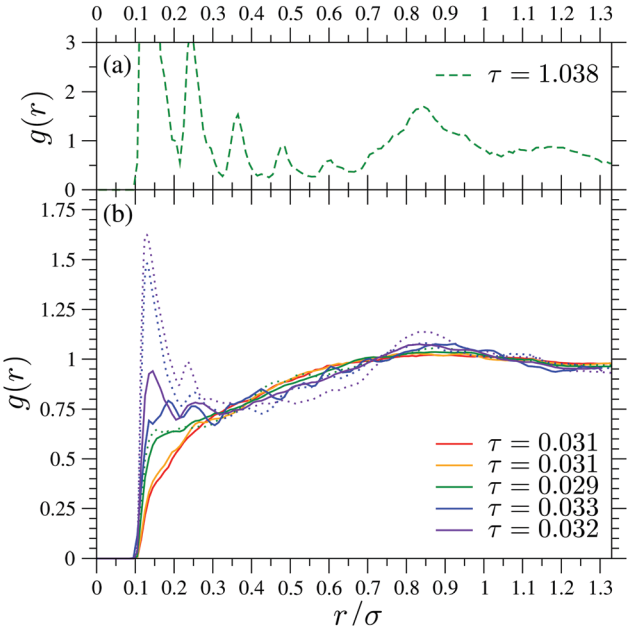

Fig. 4 (a) Positional pair correlation function $g(r)$ calculated for a system of lenses with $\kappa \simeq 0.094$ in the C solid phase at $P^* = 350$. The dashed curve refers to a system of $N = 432$ lenses and was calculated at the end of the corresponding MC run shown in Fig. 3. (b) Positional pair correlation function $g(r)$ calculated for a system of lenses with $\kappa \simeq 0.094$ in a nematic state at several values of P^*: 250 (red or gray); 300 (orange or light gray); 350 (green or gray dotted and full); 400 (blue or dark gray dotted and full); 450 (indigo or dark gray dotted and full). The dotted curves refer to a system of $N = 432$ lenses and were calculated at the beginning of the corresponding MC run shown in Fig. 3. The full curves refer to a system of $N = 864$ lenses and were calculated during a MC run like the one shown in Fig. 3. In (a) and (b) the legends give corresponding values of τ.

very rapid for a system with $N = 108$ lenses, it requires approximately 20×10^6 MC cycles to occur for a system with $N = 432$ lenses, while it is apparently suppressed for a system with $N = 864$ lenses, at least for a run length of 50×10^6 MC cycles. It seems possible to keep, at least for a number of MC cycles of the order of 10^7, a system of these lenses in a very dense nematic state, providing its size is large enough.

It becomes of interest to examine the graphs of the positional pair correlation functions $g(r)$. Fig. 4 compares the $g(r)$ in the N fluid phase at $P^* = 200$, where it is known that the crystal is even mechanically unstable, with the $g(r)$ at various larger values of P^*, calculated either at the beginning of the lengthy MC runs, when a not-large-enough system is anyway far from having reached a well-defined crystal, or for a large-enough system apparently unable to fully crystallise, along with the $g(r)$ in the C solid phase. While at $P^* = 250$ and 300 the $g(r)$ shows a typical (discotic) N fluid phase form, at higher dimensionless pressure it starts to develop new peaks at very short distance whose abscissae coincide with those of the $g(r)$ peaks in the C solid phase. It seems as the $g(r)$ at higher P^*'s is one of a state where the process that would ultimately lead to the formation of a crystal is only at a very primordial stage. This is reflected in the values of τ (Fig. 4) essentially coincident with those for the nearby N fluid phase and much smaller than those for the C solid phase.

These considerations are supported by the graphs of the bond-orientational pair correlation function $G_2^{\hat{\mathbf{r}}}(r)$ (Fig. 5). The form of this function for the metastable nematic states is very much similar to that of this function for the nearby N fluid phase: it generally decays monotonically without displaying the short-range wavy structure that characterises the form of this function for the C solid phase. Yet, a local small peak appears at $r \simeq 0.25\sigma$ in the graph of $G_2^{\hat{\mathbf{r}}}(r)$ at $P^* = 450$: its abscissa exactly corresponds to the one of the second peak in the $G_2^{\hat{\mathbf{r}}}(r)$ of the C solid phase.

The behaviour observed for these very flat lenses is analogous to that observed for hard spheres, the only difference being that the high-volume-fraction positionally disordered states are nematic for lenses with $\kappa \simeq 0.094$. Both for these very flat lenses and hard spheres, the high-volume-fraction part of the positionally disordered equation of state is, ultimately, unstable with respect to crystallisation.[46,47] If one succeeds to avoid full crystallisation, the $\frac{\varrho}{\beta P}$ *versus* ϕ curve for hard spheres too shows a 'downturn' at ~ 0.58 and then proceeds linearly until the MRJ state is reached at $\phi_{\mathrm{MRJ}} \sim 0.64$.[46] This 'downturn' corresponds to the system becoming glassy and was often considered as the signature of the system undergoing a thermodynamic (higher-order) transition from the fluid to a glassy phase.

Published on 26 September 2018. Downloaded by Princeton University on 10/22/2018 1:56:48 PM.

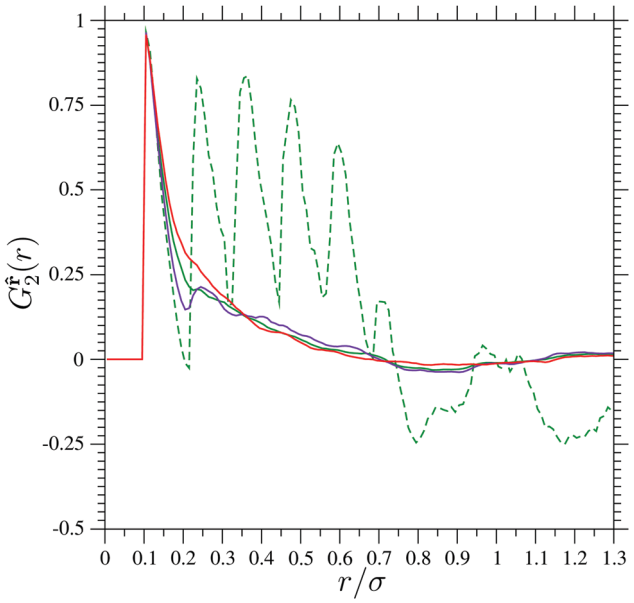

Fig. 5 Bond-orientational pair correlation function $G_2^{\hat{\mathbf{r}}}(r)$ calculated for a system of lenses with $\kappa \simeq 0.094$ in a nematic state at $P^* = 250$ (red or gray full), 350 (green or gray full) and 450 (indigo or dark gray full), and in the C solid phase at $P^* = 350$ (green or gray dashed).

The local maximum in the $\frac{\varrho}{\beta P}$ *versus* ϕ curve of lenses such as those with $\kappa \simeq 0.094$ might serve as a sort of counterexample: the $\frac{\varrho}{\beta P}$ *versus* ϕ curve showing a complete downturn at $\phi \sim 0.15$ without this being accompanied by any phase transition: the system remains in the N fluid phase. The system of lenses with $\kappa \simeq 0.094$ seems to offer another sort of counterexample. It is often stated that metastable fluid systems approaching the glass transition do not show any clear-cut changes in their structure. This statement is mostly based on results for the $g(r)$ of systems of hard or soft spherical particles. Possibly just because of their pronounced non-spherical shape, very flat lenses that approach a (nematic) glass transition do show visible changes in the form of their $g(r)$: peaks or plateaus at very short range, absent in the pair correlation functions of the nearby N fluid phase, start to develop at the abscissae in strict correspondence with those of the first peaks of the crystal $g(r)$. Thus, these (nematic) glassy states would appear as having a structure which is locally reminiscent of that characteristic of the crystal phase, as already observed, *e.g.*, for systems of hard polyhedra,[48] but has been unable to globally transform into the latter.

The overall behaviour observed for lenses with $\kappa \simeq 0.094$ and $\kappa \simeq 0.29$ also occurs for moderately thicker lenses. It is well known that the I–N phase transition shifts to progressively larger values of ϕ as κ increases. The approximate value of ϕ at which a 'downturn' is observed remains rather unaltered instead: $\tilde{\phi} \sim 0.64$, in line with the nearly constancy of the values of ϕ at which the N fluid and C solid phases co-exist in equilibrium providing κ is small enough.[12] This is illustrated in Fig. 6 which repeats what is shown in Fig. 2 for lenses with $\kappa \simeq 0.29$ but with the addition of the data collected for lenses with $\kappa \simeq 0.41$ and $\kappa \simeq 0.48$. One can note that, as the 'downturn' is approached, the respective values of $\frac{\varrho}{\beta P}$ at the same value of ϕ approach one another while beyond the 'downturn' they nearly coincide and the three curves behave essentially linearly. By carrying out the same, free-volume-theory-inspired, linear fit restricted to values of $\frac{\varrho}{\beta P}$ corresponding to $\phi > 0.65$, the following estimates for the nematic state highest volume fraction have been obtained: $\phi_{\max_N} = 0.728 \pm 0.005$ for $\kappa \simeq 0.41$ and 0.724 ± 0.005 for $\kappa \simeq 0.48$.

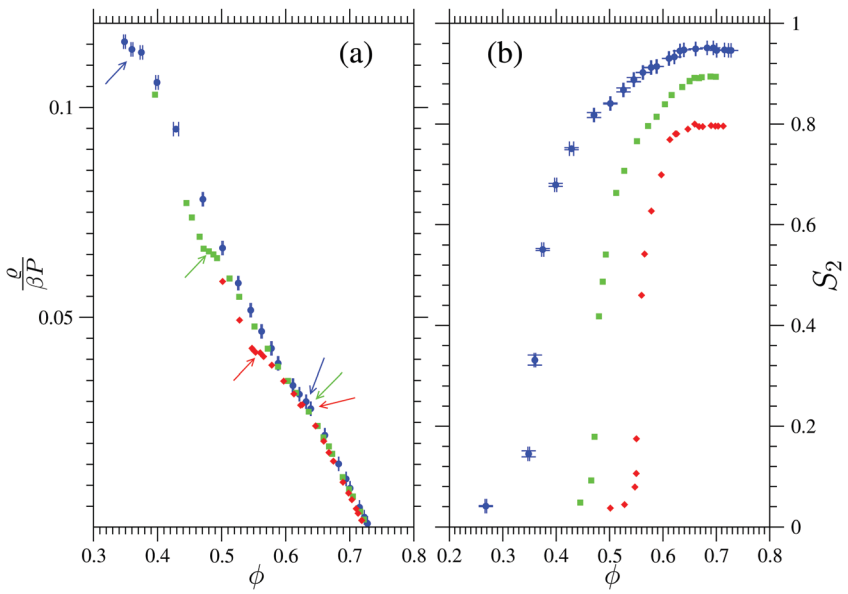

Fig. 6 (a) Inverse compressibility factor $\frac{\varrho}{\beta P}$ as a function of volume fraction ϕ: data for $\kappa \simeq 0.29$ (blue circles), $\kappa \simeq 0.41$ (green squares), $\kappa \simeq 0.48$ (red diamonds); the arrows indicate the I–N phase transition (arrows left of the data from bottom left to top right) and the 'downturn' (arrows right of the data from top right to bottom left). (b) Corresponding data for the nematic order parameter S_2 as a function of volume fraction ϕ.

This journal is © The Royal Society of Chemistry 2018

Published on 26 September 2018. Downloaded by Princeton University on 10/22/2018 1:56:48 PM.

In analogy with what is seen in the inset in Fig. 2, one can note that, as the 'downturn' is overtaken and the $\frac{\varrho}{\beta P}$ *versus* ϕ curves enter the linear regime, the S_2 ceases to increase in a nematic-like manner and remains fixed at $\simeq 0.89$ and $\simeq 0.79$ for $\kappa \simeq 0.41$ and 0.48, respectively.

Explicitly attempted for lenses with $\kappa \simeq 0.41$ at $P^* = 100$, corresponding to $\phi = 0.6160 \pm 0.0002$, for more than 50×10^6 MC cycles, full crystallisation was not observed for such moderately flat lenses. Besides the larger number of particles used, 1728 for $\kappa \simeq 0.41$ and 1920 for $\kappa \simeq 0.48$, a parameter previously seen to markedly affect the crystallisation 'time'-scale, this lack may also be ascribed to the significantly smaller value of S_2 that characterises the very dense nematic states of such moderately flat lenses: in their C solid phase, these lenses keep being nearly parallel;[12] qualitatively, it is reasonable to expect that they will strive more and more to organise into crystalline configurations starting from nematic configurations where they are not sufficiently well-aligned.

None the less, the approach of the nematic to the crystal phase and the concomitant 'downturn' and ensuing linear behaviour in the $\frac{\varrho}{\beta P}$ *versus* ϕ curve affect the form of the relevant $g(r)$'s as well as $G_2^{\hat{\mathbf{r}}}(r)$'s in a manner similar to the one already commented for lenses with $\kappa \simeq 0.094$. This is illustrated in Fig. 7 where it is seen that, similarly to what is observed in Fig. 4, the $g(r)$ develops a peaklet/shoulder at very short distance as the 'downturn' is approached and overtaken. This qualitative difference between the form of the $g(r)$ of a thermodynamically

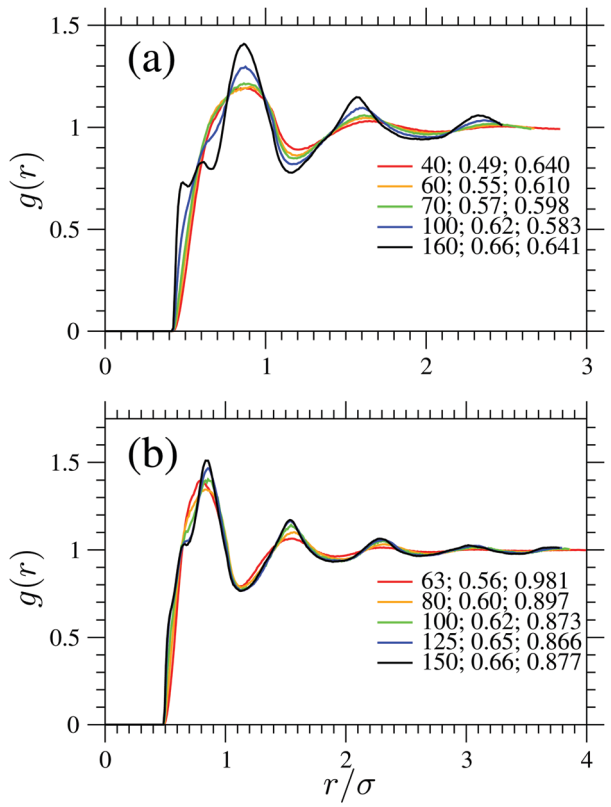

Fig. 7 (a) Positional pair correlation function $g(r)$ calculated for a system of lenses with $\kappa \simeq 0.41$ at several values of P^* =: 40, $\phi = 0.49$ (red or gray); 60, $\phi = 0.55$ (orange or light gray); 70, $\phi = 0.57$ (green or very light gray); 100, $\phi = 0.62$ (blue or dark gray); 160, $\phi = 0.66$ (black). The third number in each legend is the corresponding value of τ. (b) Positional pair correlation function $g(r)$ calculated for a system of lenses with $\kappa \simeq 0.48$ at several values of P^* =: 63, $\phi = 0.56$ (red or gray); 80, $\phi = 0.60$ (orange or light gray); 100, $\phi = 0.62$ (green or very light gray); 125, $\phi = 0.65$ (blue or dark gray); 150, $\phi = 0.66$ (black). The third number in each legend is the corresponding value of τ.

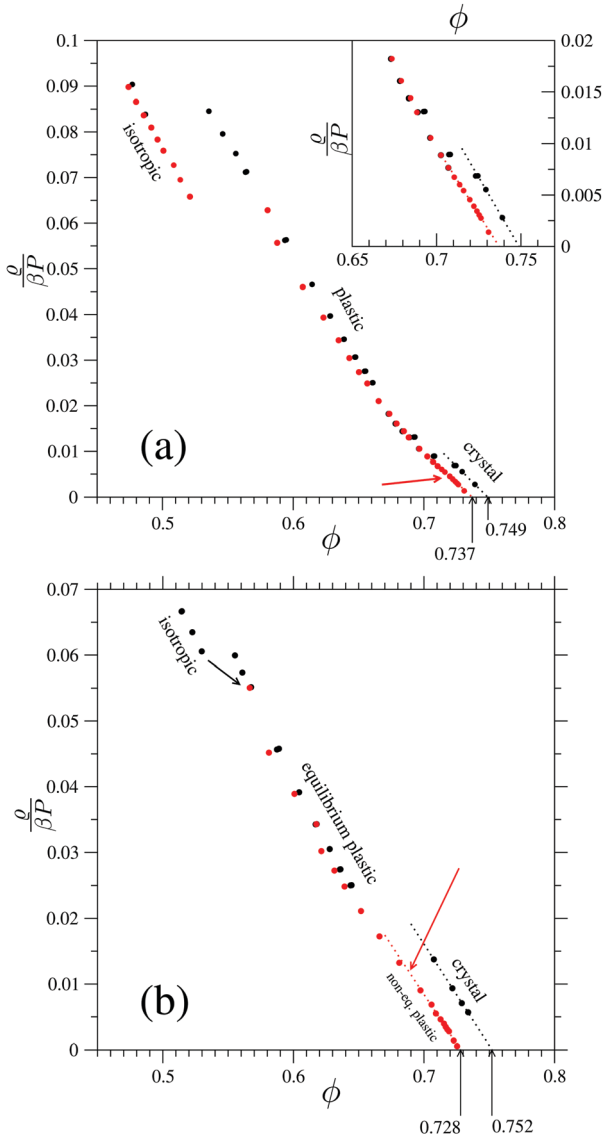

Fig. 8 Inverse compressibility factor $\frac{\varrho}{\beta P}$ as a function of volume fraction ϕ for lenses with $\kappa \simeq 0.87$ (a) and for lenses with $\kappa \simeq 0.75$ (b). Shown are the equilibrium branches obtained by progressive decompression starting from a densest-known orthorhombic configuration (black circles) and the (non-)equilibrium branches obtained by progressive compression starting from a dense isotropic configuration (red or gray circles). The dotted curves are linear, free-volume-theory-inspired, fits over the densest state points. The red (gray) arrow approximately indicates the 'downturn' and setting in of this linear behaviour in the compression curve. In (a), the top-right inset zooms in on the high-volume-fraction data. In (b), the black arrow joins that initial isotropic state point with the successive plastic state point.

Published on 26 September 2018. Downloaded by Princeton University on 10/22/2018 1:56:48 PM.

stable N fluid phase and that of the $g(r)$ of a dense nematic state, metastable with respect to crystallisation, though still appreciable, does attenuate as κ increases, being the abscissa of the first peaklet/shoulder progressively closer to that of the next highest peak. This fading sensitivity of the $g(r)$ is in line with its notorious refractoriness to show any distinct signature of glassiness in a system of spherical particles. It is of interest to observe how the values of τ reflect these changes in the form of $g(r)$ as the 'downturn' is approached and overtaken: its decreasing trend with ϕ in the nearby N fluid phase and metastable nematic state is reverted as the system becomes glassy, in keeping with the fact that τ takes larger values in the C solid phase.

Based on all these data, one can imagine that there will soon be a specific value of κ at which the I–N phase transition would occur at values of ϕ at which the 'downturn' and the ensuing linear behaviour in the $\frac{\varrho}{\beta P}$ *versus* ϕ curve also would. Before addressing this delicate regime, one can overtake it by considering large enough values of κ that correspond to 'globular' lenses. In this way, the regime of 'intermediate' lenses can be closed in from both, 'flat'- and 'globular'-lense, sides.

B. 'Globular' lenses

The analogous graphs of Fig. 2(a) and 6 for lenses with $\kappa \simeq 0.87$ and $\kappa \simeq 0.75$ are given in Fig. 8. By adopting the same compression protocol, the system rather promptly forms a P solid phase in both cases. This is analogous to what occurs for hard sphere systems whose propensity to crystallise is known.[46,47] By compressing the system further, one can follow the P solid branch until reaching those values of ϕ at which a transition to a C solid phase would occur in equilibrium. However, the P solid phase does not appear to be prone to fully crystallise in both cases. Rather, the $\frac{\varrho}{\beta P}$ *versus* ϕ curves show a tenuous by still visible 'downturn', at $\tilde{\phi} \sim 0.71$ for $\kappa \simeq 0.87$ and $\tilde{\phi} \sim 0.69$ for $\kappa \simeq 0.75$, followed by the onset of a linear, free-volume-theory-style, behaviour. By carrying out the same, free-volume-theory-inspired, linear fit, the values of the plastic state highest volume fraction obtained have been: $\phi_{\max_p} = 0.737 \pm 0.003$ for $\kappa \simeq 0.87$ and 0.728 ± 0.005 for $\kappa \simeq 0.75$.

The situation met for 'globular' lenses parallels the one met for 'flat' lenses: the 'downturn' and ensuing linear behaviour occur at values of ϕ very close to those at which the C solid would be the thermodynamically stable phase. However, the latter

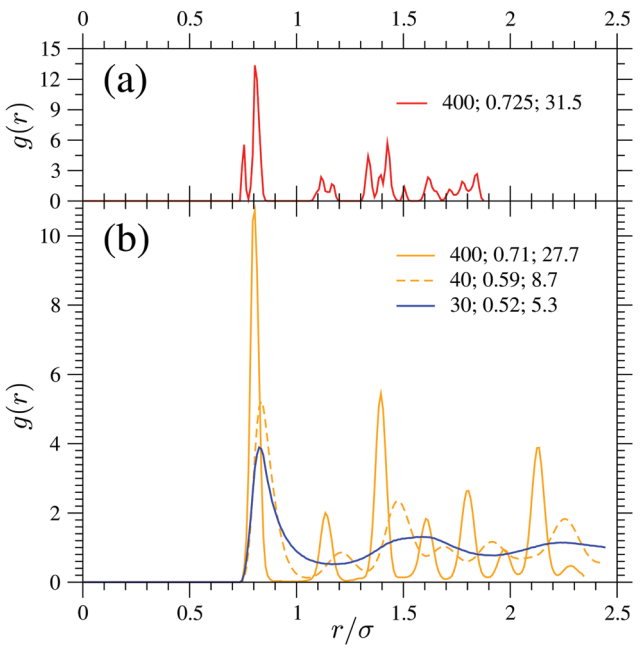

Fig. 9 (a) Positional pair correlation function $g(r)$ for a system of lenses with $\kappa \simeq 0.87$ in the C solid phase at $P^* = 400$, $\phi = 0.725$. (b) Positional pair correlation function $g(r)$ for a system of lenses with $\kappa \simeq 0.87$ in the P solid phase at $P^* = 400$, $\phi = 0.71$ (orange or light gray full line) and $P^* = 40$, $\phi = 0.59$ (orange or light gray dashed line) and in the I fluid phase at $P^* = 30$, $\phi = 0.52$ (blue or dark gray full line). The third number in each legend gives the corresponding value of τ.

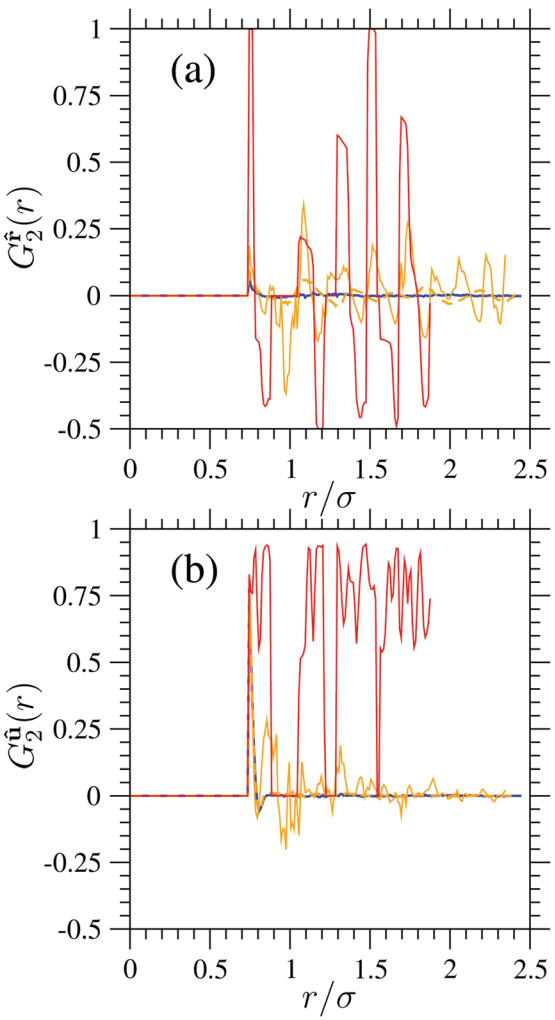

Fig. 10 Bond-orientational pair correlation function $G_2^{\hat{\mathbf{r}}}(r)$ (a) and orientational pair correlation function $G_2^{\hat{\mathbf{u}}}(r)$ (b) for a system of lenses with $\kappa \simeq 0.87$ in the C solid phase at $P^* = 400$, $\phi = 0.725$ (red or gray wavy full line), in the P solid phase at $P^* = 400$, $\phi = 0.71$ (orange or light gray full line) and $P^* = 40$, $\phi = 0.59$ (orange or light gray dashed line) and in the I fluid phase at $P^* = 30$, $\phi = 0.52$ (blue or dark gray vanishing full line).

This journal is © The Royal Society of Chemistry 2018

Published on 26 September 2018. Downloaded by Princeton University on 10/22/2018 1:56:48 PM.

does not form, completely and sufficiently readily; it is understandably difficult for the system to globally organise spontaneously at such high volume fractions so as to simultaneously satisfy the strict requirements of both positional and orientational orderings. By comparing the $g(r)$ of the P solid and C solid phase (Fig. 9), the passage from the former to the latter corresponds to a sequence of peak splittings, to begin with the peak at the shortest distances $r \simeq 0.8\sigma$: such changes in the translational degrees of freedom being impossible without proper coordinated assistance of the rotational degrees of freedom. In fact, while bond-orientational order is present [Fig. 10(a)], the orientational order keeps being absent in a P solid phase [Fig. 10(b)] and the glassy states that then form are orientational. Besides the tenuous 'downturn' and setting in of a linear behaviour in the $\frac{\varrho}{\beta P}$ *versus* ϕ curve, the formation of these orientational glassy states is signalled by the progressive slowing-down and freezing-in of the nematic director rotations.

C. 'Intermediate' lenses

With the pieces of information acquired on the state behaviour under slow compression of systems of 'flat' and 'globular' lenses, able to readily form a N fluid phase and a P solid phase, respectively, one can turn to considering 'intermediate' lenses with a value of $\kappa \in [0.5,0.7]$ whose capability of forming either mesophase is diminished or missing.[12] In these cases, it is useful to explicitly consider both small systems with $N = \mathcal{O}(10^2)$ and larger systems with $N = \mathcal{O}(10^3)$.

For systems of lenses with $\kappa \simeq 0.53$ and $\kappa = 1/\sqrt{3} \simeq 0.58$, the equation of state and the S_2 *versus* ϕ curve are given in Fig. 11. In equilibrium, *i.e.* under infinitesimally slow compression, these lenses would show a transition from a I fluid phase direct to a C solid phase. Under slow, but *a fortiori* finitely so, compression, lenses with $\kappa \simeq 0.53$ proved still able to show an I–N phase transition. This occurs at $\phi_{IN} \simeq 0.60$, a value that lies within the I–C co-existence region in the equilibrium phase diagram.[12] Despite the data for the equation of state calculated for two system sizes overlapping, the two sizes differ in the number of MC cycles required for nematic ordering to establish and the values of S_2 reached. While a system with $N = 288$ lenses required 10^6 MC cycles to see nematic ordering grow out of the isotropic state and reach a value of $S_2 \simeq 0.60$ at $P^* = 90$, a system with $N = 2304$ lenses could only reach a value of $S_2 \simeq 0.40$ after 7×10^6 MC cycles at the same dimensionless pressure. One can imagine that, if the compression of this larger system were sufficiently fast so as not to allow a transition to a nematic state to occur, slightly less dense states with (essentially) no nematic order could be obtained whose compression could proceed until they jammed. This would be consistent with the possibility, for a many hard-particle system, to reach jammed states with different value of density and varying degree of order, depending on the details of the adopted compression protocol:[6] in the present case, positionally disordered jammed states with a variable degree of orientational order. This possibility is well illustrated by systems of lenses with $\kappa = 1/\sqrt{3} \simeq 0.58$. While a system with $N = 108$ lenses keeps

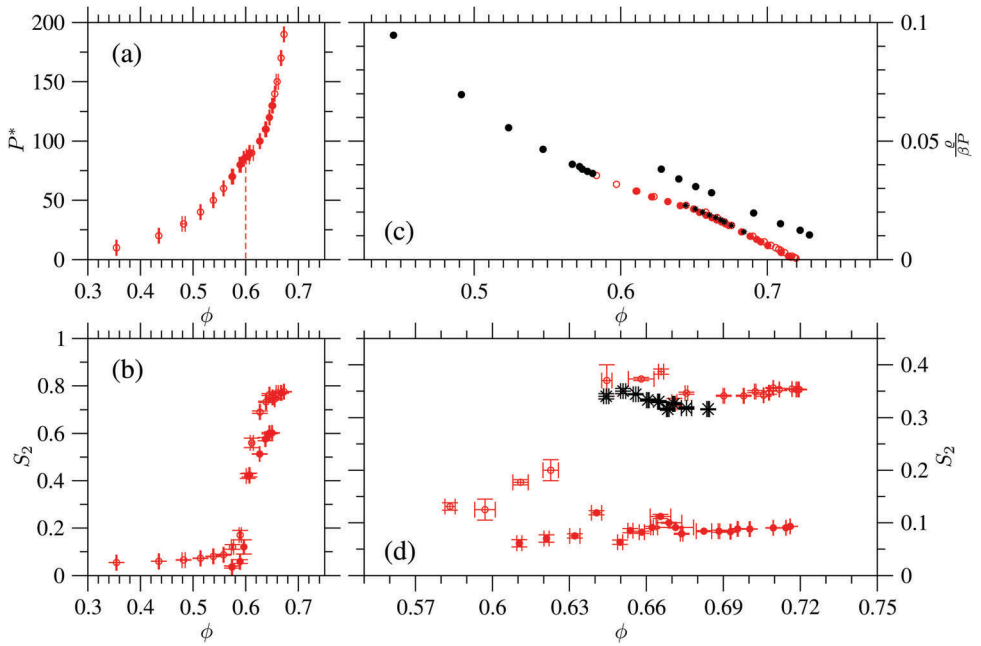

Fig. 11 Dimensionless pressure P^* (a) and nematic order parameter S_2 (b) *versus* volume fraction ϕ for lenses with $\kappa \simeq 0.53$ and $N = 288$ (empty circles) and $N = 2304$ (filled circles); in (a) the dashed line approximately locates the I–N phase transition. Inverse compressibility factor $\frac{\varrho}{\beta P}$ (c) and nematic order parameter S_2 (d) *versus* volume fraction ϕ for lenses with $\kappa = 1/\sqrt{3} \simeq 0.58$ and $N = 108$ (red or gray empty circles) and $N = 864$ as obtained by compressing either from a dense isotropic configuration (red or gray filled circles) or a configuration generated by doubling along each of the three directions of the laboratory frame of reference a previously obtained configuration with $N = 108$ (black asterisks); in (c) data obtained by decompression starting from the densest-known orthorhombic configuration are also included (black filled circles).

Published on 26 September 2018. Downloaded by Princeton University on 10/22/2018 1:56:48 PM.

being able to show an I–N phase transition at $\phi_{IN} \simeq 0.64$, *i.e.* deep into the region of the equilibrium phase diagram where the C solid is the thermodynamically stable phase, and reach a value of $S_2 \simeq 0.35$, a system with $N = 864$ lenses, despite runs as long as 80×10^6 MC cycles, remains positionally and orientationally disordered and jams at $\phi_{max_I} = 0.719 \pm 0.004$. However, if one generates a configuration with $N = 864$ lenses by doubling one with $N = 108$ and $S_2 \simeq 0.35$ along each of the three directions of the laboratory frame of reference and compresses it slowly, a slightly larger value of ϕ at jamming can be obtained while keeping the system structure nematic: $\phi_{max_N} = 0.722 \pm 0.002$. Even for a small system with $N = 108$, no full crystallisation has been observed for lenses with $\kappa = 1/\sqrt{3} \simeq 0.58$. Explicitly attempted at $P^* = 120$, corresponding to $\phi = 0.643 \pm 0.001$, and $P^* = 200$, corresponding to $\phi = 0.6737 \pm 0.0002$, the system remained positionally disordered in runs up to 80×10^6 MC cycles long. Based on the above-presented results for 'flat' lenses, it is presumable that larger systems of lenses with $\kappa = 1/\sqrt{3} \simeq 0.58$ too will fail to fully crystallise during as long MC runs.

On the lower side of the sub-interval $\kappa \in [0.5,0.7]$ then, though nematisation becomes more and more laborious as κ moves towards inner values of this sub-interval, it none the less remains possible, a fact that, together with the apparent failure of a system of such lenses to fully crystallise even if of a small size, may allow for a tentative continuation of the I–N phase transition line(s) deep into the region of the equilibrium phase diagram where the C solid is the thermodynamically stable phase.

On the upper side of the sub-interval $\kappa \in [0.5,0.7]$, systems of lenses with $\kappa \simeq 0.70$ have been considered (Fig. 12). For a small system with $N = 108$ lenses, a P solid phase forms at $P^* = 50$ on compressing from the dense I fluid phase. For such a small system, it was even possible to observe the transition from the P solid phase to the C solid phase occur at $P^* = 200$. This is understandable in view of the decisive aid periodic boundary conditions supply to crystallisation, as previously observed for lenses with $\kappa \simeq 0.094$, together with the fact that, as κ decreases from the limiting value of 1, the P–C phase transition occurs at increasingly lower volume fractions,[12] another element that should facilitate crystallisation. However, the beneficial effect of a small N is soon lost as systems with $N = 1536$ lenses, on compressing from the dense I fluid phase, fail to even undergo a transition to the P solid phase. Without the latter's formation the C solid phase is unable to form either and the system remains isotropic (Fig. 13) until it jams at $\phi_{max_I} = 0.729 \pm 0.003$ [Fig. 12(c)]. On increasing P^*, the difference in the value of ϕ between the I fluid and P solid phases progressively diminishes [Fig. 12(b)] so that it is reasonable to assume that plastic states would have jammed at a value ϕ_{max_P} only slightly larger than ϕ_{max_I}.

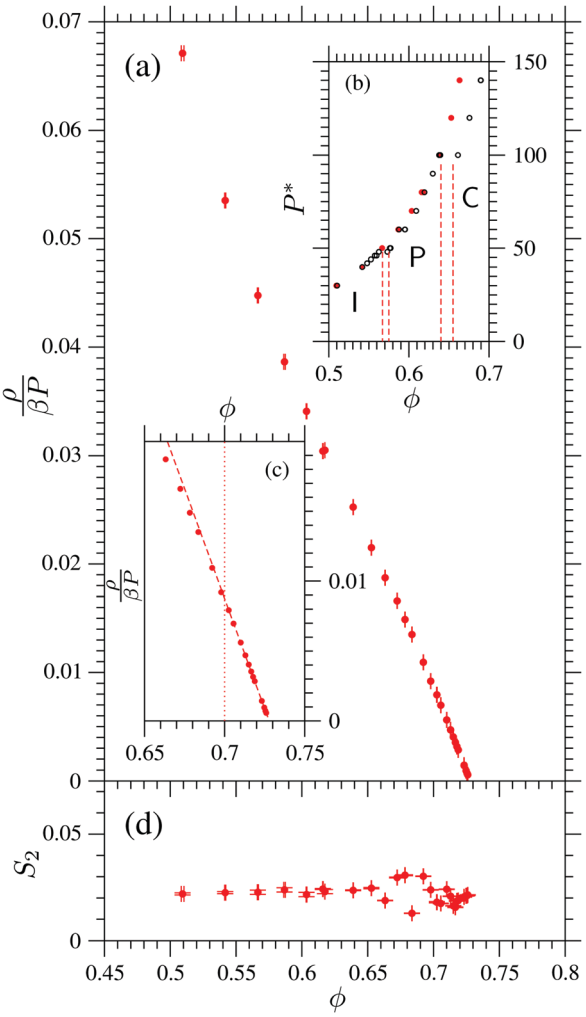

Fig. 12 (a) Inverse compressibility factor $\frac{\varrho}{\beta P}$ as a function of volume fraction ϕ for lenses with $\kappa \simeq 0.70$; the upper inset (b) compares the dimensionless pressure P^* obtained on compression starting from the I fluid phase (filled circles) with that obtained on decompression starting from a densest-known orthorhombic configuration (empty circles), with the vertical dashed lines approximately delimitating equilibrium phase boundaries; the lower inset (c) zooms in on the high-volume-fraction region, with the dotted line indicating the value of ϕ beyond which a free-volume-theory-inspired linear fit, the dashed line, was carried out. (d) Nematic order parameter S_2 as a function of volume fraction ϕ.

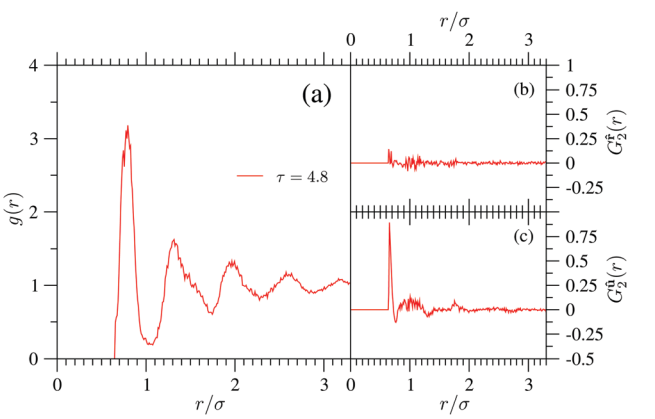

Fig. 13 Pair correlation functions calculated for a system of lenses with $\kappa \simeq 0.70$ at $P^* = 5000$ corresponding to $\phi = 0.7260 \pm 0.0001$: (a) positional $g(r)$ with the legend giving the corresponding value of τ; (b) bond-orientational $G_2^{\mathbf{r}}(r)$; (c) orientational $G_2^{\mathbf{q}}(r)$.

This journal is © The Royal Society of Chemistry 2018

Published on 26 September 2018. Downloaded by Princeton University on 10/22/2018 1:56:48 PM.

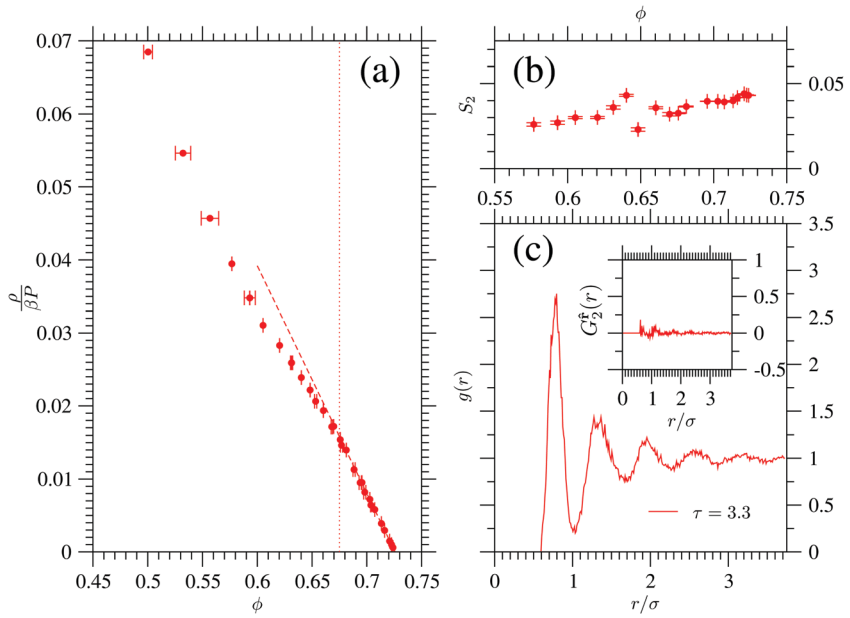

Fig. 14 (a) Inverse compressibility factor $\frac{\varrho}{\beta P}$ as a function of volume fraction ϕ for lenses with $\kappa \simeq 0.63$; the dotted line indicates the value of ϕ beyond which a free-volume-theory-inspired linear fit, the dashed line, was carried out. (b) Nematic order parameter S_2 as a function of volume fraction ϕ. (c) Positional pair correlation function $g(r)$ at $P^* = 5000$ corresponding to $\phi = 0.7239 \pm 0.0001$; the legend gives the corresponding value of τ; the inset shows the corresponding bond-orientational pair correlation function $G_2^{\hat{t}}(r)$.

The difficulty experienced by an isotropic state to transit to either a nematic or plastic state as κ approaches a value of $\simeq 2/3$ makes reasonable to expect that systems of such 'intermediate' lenses jam in a positionally and orientationally disordered state even when they are slowly compressed starting from their dense I fluid phase. This is indeed what has been observed for lenses with $\kappa \simeq 0.63$ (Fig. 14). By carrying out the same, free-volume-theory-inspired, linear fit of the high-volume-fraction part of the $\frac{\varrho}{\beta P}$ *versus* ϕ curve, one obtains $\phi_{\max_I} = 0.726 \pm 0.007$.

D. Structure factor and effective hyperuniformity of the jammed states

It becomes now of interest to investigate the hyperuniformity of the generated positionally and/or orientationally disordered jammed packings by computing the structure factor $S(k)$ and examining its small-wavenumber behaviour.[26–29] Fig. 15 shows $S(k)$ for the strictly jammed packings generated for $\kappa \simeq 0.41$, $\kappa \simeq 0.70$ and $\kappa \simeq 0.87$. The $S(k)$ for the latter packing remains at values $\approx 10^{-3}$ for $1 \lesssim k\sigma \lesssim 5$ in keeping with its plastic-crystalline character. This is further evidenced by the $S(k)$ multiple peaks that extend up to large values of k. The $S(k)$ for the other two packings further demonstrates their positionally disordered character: they only have a relatively broad peak at $k\sigma \approx 10$ and then damped-oscillatorily decay to unity. Both these $S(k)$'s show very small decreasing values as $k \to 0$. The present system sizes prevent us to precisely discern whether this limiting behaviour is linear (implying power-law decay of $g(r)$ to unity) or quadratic (implying exponentially fast decay of $g(r)$ to unity): a number of particles as large as 10^6 was needed to detect a linear behaviour of $S(k)$ in MRJ packings of hard

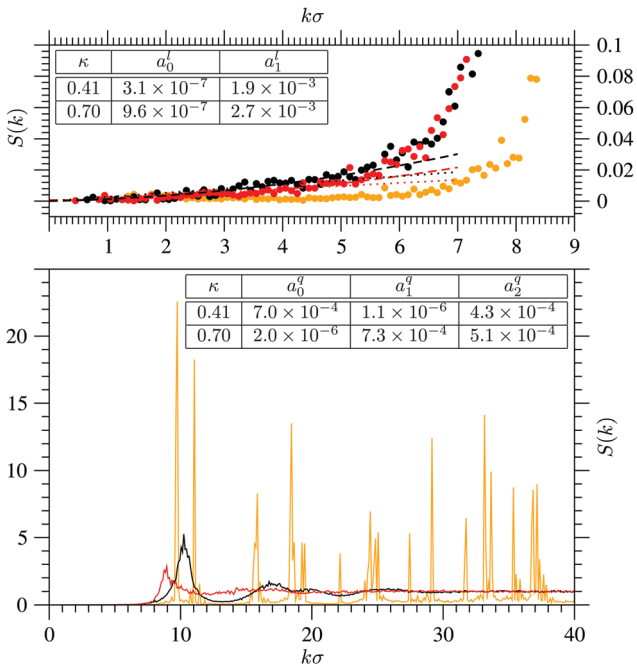

Fig. 15 The structure factor $S(k)$ for three strictly jammed packings of lenses with: $\kappa \simeq 0.41$, representative of 'flat' lens class with a nematic structure (red or gray line and red or gray circles); $\kappa \simeq 0.70$, representative of 'intermediate' lens class with an isotropic structure (black curve and black circles); $\kappa \simeq 0.87$, representative of 'globular' lens class with a plastic structure (orange or light gray curve and orange or light gray circles). The upper panel zooms in on the small-k behaviour while the two inset tables report the coefficients of the linear (dotted curve of the corresponding colour) and quadratic (dashed curve of the corresponding colour) fits over $k\sigma < 5$ for the two positionally disordered packings.

Published on 26 September 2018. Downloaded by Princeton University on 10/22/2018 1:56:48 PM.

spheres that remarkably differs from the quadratic behaviour expected in the equilibrium fluid.[49] The present system sizes appear nonetheless to be sufficiently large to qualify the two jammed packings as effectively hyperuniform to a good approximation. In fact, both the linear fit, $a_0^{\mathrm{l}} + a_1^{\mathrm{l}}k$, and the quadratic fit, $a_0^{\mathrm{q}} + a_1^{\mathrm{q}}k + a_2^{\mathrm{q}}k^2$, limited to $k\sigma < 5$, provide values for the constant term, a_0^{l} or a_0^{q}, that are $<10^{-3}$ (inset tables in Fig. 15). This differs from the equilibrium fluid where the quadratic character of the limit behaviour is clear and the value of the $\lim_{k\to 0} S(k)$ is at least one order of magnitude larger.

E. Non-crystalline state diagram

The data obtained for the estimated value of volume fraction at jamming, $\phi_{\max_{\mathrm{N}}}$, $\phi_{\max_{\mathrm{I}}}$, $\phi_{\max_{\mathrm{P}}}$, along with the additional data for the I–N phase transition line(s) can be lain over the κ–ϕ plane. In the same Fig. 16, data for ϕ_{MRJ} are also included.[50] The elements of the set $\{\phi_{\max_{\mathrm{N}}},\phi_{\max_{\mathrm{I}}},\phi_{\max_{\mathrm{P}}}\}$ show a little variability. Yet, one can recognise their increasing trend as κ moves from a minimum in the sub-interval [0.5,0.7] towards either extreme of its entire interval. One can surmise that a continuation of the I–N phase transition line(s) and that of the I–P phase transition lines[12] are compatible with their meeting at the same, singular, state point whose abscissa and ordinate are, respectively, $\kappa_{\mathrm{S}} \simeq 2/3$ and $\phi_{\mathrm{S}} \simeq 0.73$. The maximum of the ϕ_{MRJ} *versus* κ curve too is compatible with having such a value of abscissa and potentially reaching such a value of ordinate. One can then imagine a (very) ideal numerical experiment during which systems of lenses are compressed extremely slowly yet it is managed to impede the crystal phase to completely form. In that case, two curves might depart from that singular state point in a cusp-like manner: one is the curve of the values of ϕ for the jammed states with $0 \leq \kappa < \kappa_{\mathrm{S}}$ that exhibit nematic ordering; the other is the curve of the values of ϕ for the jammed states with $\kappa_{\mathrm{S}} < \kappa \leq 1$ that exhibit plastic ordering. What actually observed is not this (very) ideal situation. For values of κ in the left and right neighbourhood of κ_{S}, the jammed states obtained are isotropic: a much (painfully) slower compression protocol should have been employed while simultaneously impeding the crystal phase to completely form to see at these values of κ either nematic or plastic ordering to appear and settle. For values of κ far enough from κ_{S} though, the adopted, *a fortiori* finitely, slow compression protocol seems adequate to generate jammed state points belonging to either of these curves.

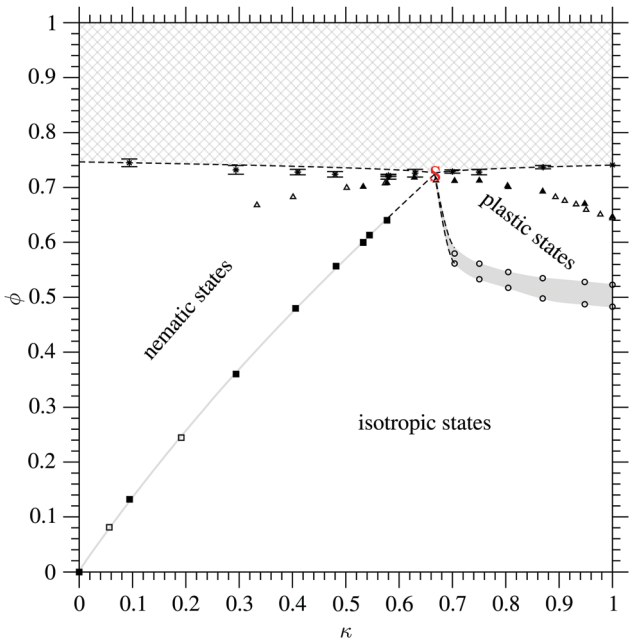

Fig. 16 Crystal-less state diagram for lenses in the plane aspect ratio κ–volume fraction ϕ. There are three regions where nematic, isotropic and plastic states are (either absolutely or relatively) stablest delimitated by: the IN phase transition line(s) and its (their) continuation (empty and filled squares crossed by the gray wide line continued by the black dashed line); the IP phase transition lines and their continuation (empty circles and the gray region within continued by the two black dashed lines); the non-crystalline jammed state volume fraction curve (black asterisks and black dashed line; above, state points within the gray netted region are unachievable). Hypothetically, the latter curve meets with both IN and IP phase transition line continuations at the singular state point marked with a red (gray) S. The triangles are data for the MRJ volume fractions of lenses (filled) and hard oblate ellipsoids[20] (empty).

IV. Conclusions

In this work, dense positionally and/or orientationally disordered, including jammed, monodisperse packings of hard convex lens-shaped particles have been generated by slow compression, *via* a Monte Carlo method based procedure, starting from relatively dense isotropic configurations and ending at corresponding effectively hyperuniform strictly jammed states.

The free-volume-theory-inspired extrapolation of the value of volume fraction at jamming together with the continuation of the I–N and I–P phase transition lines in the high-volume-fraction region where the crystal would be the thermodynamically stable phase have allowed us to sketch, in the aspect ratio–volume fraction plane, a non-crystalline state diagram. This consists of three regions, nematic, isotropic and plastic, delineated by the aforementioned phase-transition lines and their continuations as well as the bounding non-crystalline jammed state curve. The latter curve and the continuation of the phase-transition lines are compatible with their meeting at the same, singular, jammed state point located at $\kappa_{\mathrm{S}} \simeq 2/3$ and $\phi_{\mathrm{S}} \simeq 0.73$. This value of κ_{S} is also that corresponding to the maximum of the ϕ_{MRJ} *versus* κ curve.

Lenses with such an aspect ratio are special in that their MRJ states can reach the highest volume fraction while keeping a positionally and orientationally disordered structure with no propensity to densify further by separately introducing positional or orientational ordering. Thus, such unique lens packings are very good (positional and orientational) glass formers. The effective hyperuniformity of their corresponding MRJ states further contributes to their promise of being disordered materials with novel physical properties.

Ideal dense non-crystalline states are those whose tendency to crystallise is greatly suppressed. For lenses, full crystallisation

 This journal is © The Royal Society of Chemistry 2018

Published on 26 September 2018. Downloaded by Princeton University on 10/22/2018 1:56:48 PM.

was not generally observed. Systems of lenses are resistant to fully crystallise spontaneously unless three conditions are simultaneously met:

[I] the system size is sufficiently small so that periodic boundary conditions promote (crystal) ordering;

[II] a nematic or plastic mesophase preforms with a large degree of orientational or positional order: by effectively reducing the number of degrees of freedom, these mesophases act as a stepping stone towards full crystallisation; and

[III] the transition to the crystal phase occurs at a low enough volume fraction.

That these three conditions are expected to hold is consistent with previous observations for systems of hard spheres of varying dimensionality d.[51,52] Taking $d = 4$ as an example, while a system with $N = 648$ hard spheres could form the D_4 crystal phase, a system with $N = 10^4$ hard spheres did not show any recognisable sign of crystallisation on compressing from the fluid phase.[51] On increasing d, the transition to the crystal phase occurs at increasingly lower volume fractions.[51,52] However, this potentially beneficial effect is more than offset by the increasing number of degrees of freedom, making full crystallisation increasingly difficult as d increases.[51,52]

Conflicts of interest

There are no conflicts of interest to declare.

Acknowledgements

G. C. acknowledges the support of the Government of Spain under grants no. FIS2013-47350-C5-1-R, MDM-2014-0377 and FIS2017-86007-C3-1-P. S. T. was supported by the National Science Foundation under grant no. CBET-1701843.

References

1 P. M. Chaikin and T. C. Lubensky, *Principles of condensed matter physics*, Cambridge University Press, Cambridge, 1995.
2 J. A. Barker and D. Henderson, *Rev. Mod. Phys.*, 1976, **48**, 587.
3 S. Sacanna and D. J. Pine, *Curr. Opin. Colloid Interface Sci.*, 2011, **16**, 96; S. Sacanna, M. Korpics, K. Rodriguez, L. Colón-Meléndez, S. H. Kim, D. J. Pine and G. R. Yi, *Nat. Commun.*, 2013, **4**, 1688; S. Sacanna, D. J. Pine and G. R. Yi, *Soft Matter*, 2013, **9**, 8096.
4 M. P. Allen, G. T. Evans, D. Frenkel and B. M. Mulder, *Adv. Chem. Phys.*, 1993, **86**, 1.
5 *Theory and simulation of hard-sphere fluids and related systems*, ed. A. Mulero, Lect. Notes Phys., Springer, Berlin Heidelberg, 2008, vol. 753.
6 S. Torquato and F. H. Stillinger, *Rev. Mod. Phys.*, 2010, **82**, 2633.
7 L. Mederos, E. Velasco and Y. Martínez-Ratón, *J. Phys.: Condens. Matter*, 2014, **26**, 463101.
8 M. Dijkstra, *Adv. Chem. Phys.*, 2015, **156**, 35.
9 C. Avendaño and F. A. Escobedo, *Curr. Opin. Colloid Interface Sci.*, 2017, **30**, 62.
10 S. Torquato, *J. Chem. Phys.*, 2018, **149**, 020901.
11 A. P. Minton, *Biophys. J.*, 2005, **88**, 971; A. P. Minton, *J. Pharm. Sci.*, 2007, **96**, 3466.
12 G. Cinacchi and S. Torquato, *J. Chem. Phys.*, 2015, **143**, 224506.
13 M. He and P. Siders, *J. Phys. Chem.*, 1990, **94**, 7280.
14 *E.g. Introduction to Liquid Crystals*, ed. E. B. Priestley, P. J. Wojtowicz and P. Sheng, Plenum Press, New York, 1975.
15 *E.g.* L. A. K. Staveley, *Annu. Rev. Phys. Chem.*, 1962, **13**, 351.
16 D. Frenkel, B. M. Mulder and J. P. McTague, *Phys. Rev. Lett.*, 1984, **52**, 287; D. Frenkel and B. M. Mulder, *Mol. Phys.*, 1985, **55**, 1171; G. Odriozola, *J. Chem. Phys.*, 2012, **136**, 134505; G. Bautista-Carvajal, A. Moncho-Jordá and G. Odriozola, *J. Chem. Phys.*, 2013, **138**, 064501.
17 A. Donev, F. H. Stillinger, P. M. Chaikin and S. Torquato, *Phys. Rev. Lett.*, 2004, **92**, 255506.
18 S. R. Williams and A. P. Philipse, *Phys. Rev. E: Stat., Nonlinear, Soft Matter Phys.*, 2003, **67**, 051301.
19 A. Donev, I. Cisse, D. Sachs, E. A. Variano, F. H. Stillinger, R. Connelly, S. Torquato and P. M. Chaikin, *Science*, 2004, **303**, 990; W. Man, A. Donev, F. H. Stillinger, M. T. Sullivan, W. B. Russel, D. Heeger, S. Inati, S. Torquato and P. M. Chaikin, *Phys. Rev. Lett.*, 2005, **94**, 198001.
20 P. M. Chaikin, A. Donev, W. Man, F. H. Stillinger and S. Torquato, *Ind. Eng. Chem. Res.*, 2006, **45**, 6960.
21 A. Donev, R. Connelly, F. H. Stillinger and S. Torquato, *Phys. Rev. E: Stat., Nonlinear, Soft Matter Phys.*, 2007, **75**, 051304.
22 A. Wouterse, S. R. Williams and A. P. Philipse, *J. Phys.: Condens. Matter*, 2007, **19**, 406215; A. V. Kyrylyuk, M. A. Haar, L. Rossi, A. Wouterse and A. P. Philipse, *Soft Matter*, 2011, **7**, 1671; J. Zhao, S. Li, R. Zou and A. Yu, *Soft Matter*, 2012, **8**, 1003; C. Ferreiro-Córdova and J. S. van Duijneveldt, *J. Chem. Eng. Data*, 2014, **59**, 3055; L. Meng, Y. Jiao and S. Li, *Powder Technol.*, 2016, **292**, 176.
23 Y. Jiao, F. H. Stillinger and S. Torquato, *Phys. Rev. E: Stat., Nonlinear, Soft Matter Phys.*, 2010, **81**, 041304.
24 Y. Jiao and S. Torquato, *Phys. Rev. E: Stat., Nonlinear, Soft Matter Phys.*, 2011, **84**, 041309; D. Chen, Y. Jiao and S. Torquato, *J. Phys. Chem. B*, 2014, **118**, 7981.
25 S. Torquato, T. M. Truskett and P. G. Debenedetti, *Phys. Rev. Lett.*, 2000, **84**, 2064. This work introduced the concept of MRJ state for hard spheres, the suitable order metrics involved being positional and bond-orientational. The same concept is generalisable to hard non-spherical particles by adding suitable orientational order metrics.
26 S. Torquato and F. H. Stillinger, *Phys. Rev. E: Stat., Nonlinear, Soft Matter Phys.*, 2003, **68**, 041113.
27 C. Zachary and S. Torquato, *J. Stat. Mech.: Theory Exp.*, 2009, P12015.
28 S. Torquato, *Phys. Rev. E*, 2016, **94**, 022122; S. Torquato, *J. Phys.: Condens. Matter*, 2016, **28**, 414012.
29 S. Torquato, *Phys. Rep.*, 2018, **745**, 1.
30 A. Gabrielli, M. Joyce and F. Sylos Labini, *Phys. Rev. D: Part. Fields*, 2002, **65**, 083523. In the context of this work, hyperuniformity has been termed superhomogeneity.

Published on 26 September 2018. Downloaded by Princeton University on 10/22/2018 1:56:48 PM.

31 N. Metropolis, A. W. Rosenbluth, M. N. Rosenbluth, A. H. Teller and E. Teller, *J. Chem. Phys.*, 1953, **21**, 1087.
32 M. P. Allen and D. J. Tildesley, *Computer Simulation of Liquids*, Clarendon Press, Oxford, 1987; W. Krauth, *Statistical Mechanics: Algorithms and Computations*, Oxford University Press, Oxford, 2006.
33 W. W. Wood, *J. Chem. Phys.*, 1968, **48**, 415; W. W. Wood, *J. Chem. Phys.*, 1970, **52**, 729.
34 R. Najafabadi and S. Yip, *Scr. Metall.*, 1983, **17**, 1199; S. Yashonath and C. N. R. Rao, *Mol. Phys.*, 1985, **54**, 245.
35 S. Torquato and Y. Jiao, *Nature*, 2009, **460**, 876; S. Torquato and Y. Jiao, *Phys. Rev. E: Stat., Nonlinear, Soft Matter Phys.*, 2009, **80**, 041104.
36 J. Vieillard-Baron, *Mol. Phys.*, 1974, **28**, 809.
37 S. Torquato, G. Zhang and F. H. Stillinger, *Phys. Rev. X*, 2015, **5**, 021020.
38 C. Zannoni, in *The Molecular Physics of Liquid Crystals*, ed. G. R. Luckhurst and G. W. Gray, Academic Press, London, 1979, ch. 3.
39 J. G. Kirkwood, *J. Chem. Phys.*, 1950, **18**, 380; W. W. Wood, *J. Chem. Phys.*, 1952, **20**, 1334; Z. W. Salsburg and W. W. Wood, *J. Chem. Phys.*, 1962, **37**, 798.
40 F. H. Stillinger and Z. W. Salsburg, *J. Stat. Phys.*, 1969, **1**, 179; A. Donev, S. Torquato and F. H. Stillinger, *Phys. Rev. E: Stat., Nonlinear, Soft Matter Phys.*, 2005, **71**, 011105.
41 S. Torquato and F. H. Stillinger, *J. Phys. Chem. B*, 2001, **105**, 11849.
42 A. Donev, S. Torquato, F. H. Stillinger and R. Connelly, *J. Appl. Phys.*, 2004, **95**, 989; A. Donev, S. Torquato, F. H. Stillinger and R. Connelly, *J. Comput. Phys.*, 2004, **197**, 139.
43 J. M. Gordon, J. H. Gibbs and P. D. Fleming, *J. Chem. Phys.*, 1976, **65**, 2771.
44 D. Frenkel and R. Eppenga, *Phys. Rev. Lett.*, 1982, **49**, 1089; R. Eppenga and D. Frenkel, *Mol. Phys.*, 1984, **52**, 1303.
45 G. Cinacchi and A. Tani, *J. Phys. Chem. B*, 2015, **119**, 5671.
46 M. D. Rintoul and S. Torquato, *Phys. Rev. Lett.*, 1996, **77**, 4198; M. D. Rintoul and S. Torquato, *J. Chem. Phys.*, 1996, **105**, 9258.
47 J. Zhu, M. Li, R. Rogers, W. Meyer, R. H. Ottewill, STS-73 Space Shuttle Crew, W. B. Russel and P. M. Chaikin, *Nature*, 1997, **387**, 883; Z. Cheng, P. M. Chaikin, W. B. Russel, W. V. Meyer, J. Zhu, R. B. Rogers and R. H. Ottewill, *Mater. Des.*, 2001, **22**, 529; Z. Cheng, P. M. Chaikin, J. Zhu, W. B. Russel and W. V. Meyer, *Phys. Rev. Lett.*, 2002, **88**, 015501.
48 P. F. Damasceno, M. Engel and S. C. Glotzer, *Science*, 2012, **337**, 453.
49 A. Donev, F. H. Stillinger and S. Torquato, *Phys. Rev. Lett.*, 2005, **95**, 090604.
50 In Fig. 16 the ϕ_{MRJ} *versus* κ data for hard oblate ellipsoids[20] are also included. One can note that the ϕ_{MRJ} for hard oblate ellipsoids tend to be slightly lower than the corresponding quantity for lenses at the same value of κ. This is in line with lenses' capability of generally packing more densely than do hard (prolate and oblate) ellipsoids.[12].
51 M. Skoge, A. Donev, F. H. Stillinger and S. Torquato, *Phys. Rev. E: Stat., Nonlinear, Soft Matter Phys.*, 2006, **74**, 041127.
52 J. A. van Meel, D. Frenkel and P. Charbonneau, *Phys. Rev. E: Stat., Nonlinear, Soft Matter Phys.*, 2009, **79**, 030201(R); J. A. van Meel, B. Charbonneau, A. Fortini and P. Charbonneau, *Phys. Rev. E: Stat., Nonlinear, Soft Matter Phys.*, 2009, **80**, 061110; P. Charbonneau, A. Ikeda, G. Parisi and F. Zamponi, *Phys. Rev. Lett.*, 2011, **107**, 185702.

 This journal is © The Royal Society of Chemistry 2018